Electronic Supplementary Material (ESI) for Dalton Transactions.
This journal is © The Royal Society of Chemistry 2016

Supporting Information for

A Series of Robust Metal-Porphyrinic Frameworks Based on Rare Earth Clusters and Their Application in N-H Carbene Insertion

Lei Xu,[a] Meng-Ke Zhai,[a] Fei Wang,[a] Lin Sun,[a] Hong-Bin Du[a*]

[a] State Key Laboratory of Coordination Chemistry, Collaborative Innovation Center of Chemistry for Life Sciences, School of Chemistry and Chemical Engineering, Nanjing University, Nanjing, 210023, China. E-mail: hbdu@nju.edu.cn

Table of Contents

S1. Chemicals and instrumentation.

Commercially available reagents were purchased as analytical grade and used without further purification unless otherwise stated. Porphyrinic ligands tetrakis(4-carboxyphenyl)porphyrin (TCPP) and tetra-phenylporphyrin (TPP) were prepared according to the reported procedures.[1] Fe(TPP)Cl was synthesized via the method reported in literatures.[2] Pyrrole was purchased from Aladdin Inc., Yttrium nitrate hexahydrate ($Y(NO_3)_3{\cdot}6H_2O$, 99.95% REO), Gadolinium nitrate hexahydrate ($Gd(NO_3)_3{\cdot}6H_2O$, 99.95% REO), Terbiumnitrate hexahydrate ($Tb(NO_3)_3{\cdot}6H_2O$, 99.99% REO), Dysprosiumnitrate hexahydrate ($Dy(NO_3)_3{\cdot}6H_2O$, 99.99% REO), Erbium nitrate pentahydrate ($Er(NO_3)_3{\cdot}5H_2O$, 99.99% REO), Ytterbium nitrate pentahydrate ($Yb(NO_3)_3{\cdot}5H_2O$, 99.99% REO) were obtained from Energy Chemical; 2-fluorobenzoic acid was obtained from J&K Scientific; 4-fluoroaniline, 4-chloroaniline, 4-bromoaniline, 4-nitroaniline, *p*-toluidine, 4-aminobenzonitrile, 4-(trifluoromethyl)aniline were purchased from Heowns Biochemical Technology Co., Ltd. Other reagents were purchased from Sinopharm Chemical Reagent Co., Ltd.

Powder X-ray diffraction (PXRD) measurements were performed on a Bruker D8-Advance diffractometer with a Cu sealed tube (λ = 1.54178 Å) at 40 kV and 40 mA. Elemental analysis (C, H and N) was performed by an Elementar Vario EL III element analyzer. Thermogravimetry analysis (TGA) was conducted on a Mettler-Toledo (TGA/DSC1) thermal analyzer under N_2 atmosphere with a heating rate of 10 °C /min. Fourier transform infrared spectra (FT-IR) were recorded as KBr pellets on a Bruker Tensor 27 FT-IR spectrometer. Proton nuclear magnetic resonance (^{1}H NMR) data were collected on Bruker Avance 300MHz spectrometer. The UV-Vis spectra were recorded on Varian Cary 5000 UV-Vis-NIR spectrophotometer using $BaSO_4$ as reference. Inductively Coupled Plasma Optical Emission Spectrometry (ICP-OES) was obtained on Perkin Elmer Optima 5300DV. Supercritical Fluid Technologies (SFT) HPR-100 reactor was used to perform supercritical CO_2 activation of the sample. Gas adsorption isotherms were collected by a volumetric method on a Micromeritics ASAP 2020 sorption analyzer, N_2 adsorption isotherms were measured at 77 K.

S2. Synthesis of NUPF-2M (M = Y, Gd, Tb, Dy, Er, Yb) crystals

All the target single crystals of NUPF-2M were obtained by using similar solvothermal method, therefore only the preparation of NUPF-2Y as a representative is described in detail.

NUPF-2Y: TCPP (10 mg, 0.012 mmol) and 2-fluorobenzoic acid (1 g, 7.14 mmol) were added into *N,N*-dimethylformamide (DMF, 2 mL) in a small capped vial and sonicated for ten minutes for dissolution. 0.5 mL deionized water and 38 mg of $Y(NO_3)_3{\cdot}6H_2O$ (0.1 mmol, 45 mg for $Gd(NO_3)_3{\cdot}6H_2O$, $Tb(NO_3)_3{\cdot}6H_2O$, $Dy(NO_3)_3{\cdot}6H_2O$, $Er(NO_3)_3{\cdot}5H_2O$ and $Yb(NO_3)_3{\cdot}5H_2O$, respectively) were added into the above solution and further sonicated for ten minutes. The vial was placed into a Teflon lined acid-digestion bomb and heated at 120°C for 3 days, then it was allowed to cool to room temperature naturally. Small hexagonal-prism shaped crystals of NUPF-2Y were obtained followed by washing several times with DMF, ethanol and anhydrous ether, respectively. Yield: ~15.5 mg (78 %, based on porphyrin). Anal. Calcd for $C_{144}H_{97}N_{12}O_{41}Y_9{\cdot}5H_2O{\cdot}12DMF$: C, 48.93; H, 4.36; N, 7.61 %, Found: C, 48.87; H, 4.62; N, 8.04 %. The overall formula of NUPF-2Y was determined by X-ray crystallography, elemental analysis, and thermogravimetric analysis. FT-IR (KBr pellet, cm^{-1}): v=3419(s), 1661(m), 1601(s), 1534(m), 1412(s), 1180(w), 1147(w), 1102(m), 1019(w), 963(m), 851(w), 797(w), 776(w),723(m), 483(m).

NUPF-2Gd: Yield: ~16 mg (81 %, based on porphyrin). Anal. Calcd for $C_{144}H_{97}N_{12}O_{41}Gd_9{\cdot}9H_2O{\cdot}15DMF$: C, 42.63; H, 4.16; N, 7.10 %, Found: C, 42.87; H, 4.57; N, 7.84 %. The overall formula of NUPF-2Gd was determined by X-ray crystallography, elemental analysis, and thermogravimetric analysis. FT-IR (KBr pellet, cm^{-1}): v = 3416(s), 3131(m), 1607(m), 1540(s), 1415(s), 1186(w), 1153(w), 1107(w), 1022(w), 963(s), 865(w), 806(m), 770(m), 728(m), 482(m).

NUPF-2Tb: Yield: ~16 mg (81 %, based on porphyrin). Anal. Calcd for $C_{144}H_{97}N_{12}O_{41}Tb_9{\cdot}9H_2O{\cdot}10DMF$: C, 43.26; H, 3.86; N, 6.38 %, Found: C, 43.67; H, 4.23; N, 6.74 %. The overall formula of NUPF-2Tb was determined by X-ray crystallography, elemental analysis, and thermogravimetric analysis. FT-IR (KBr pellet, cm^{-1}): v = 3392(s), 1612(m), 1536(m), 1408(s), 1183(w), 1107(w), 1022(w), 963(m), 852(w), 806(w), 773(w), 721(m), 485(m).

NUPF-2Dy: Yield: ~14 mg (71 %, based on porphyrin). Anal. Calcd for

$C_{144}H_{97}N_{12}O_{41}Dy_9 \cdot 6H_2O \cdot 7DMF$: C, 41.87; H, 3.36; N, 5.62 %, Found: C, 42.27; H, 3.73; N, 6.04 %. The overall formula of NUPF-2Dy was determined by X-ray crystallography, elemental analysis, and thermogravimetric analysis. FT-IR (KBr pellet, cm^{-1}): ν = 3419(s), 3131(m), 1609(m), 1539(m), 1402(s), 1173(w), 1022(w), 968(m), 858(w), 796(w), 773(w), 725(w), 485(m).

NUPF-2Er: Yield: ~17 mg (85 %, based on porphyrin). Anal. Calcd for $C_{144}H_{97}N_{12}O_{41}Er_9 \cdot 6H_2O \cdot 9DMF$: C, 41.72; H, 3.52; N, 5.98 %, Found: C, 41.53; H, 3.68; N, 6.35 %. The overall formula of NUPF-2Er was determined by X-ray crystallography, elemental analysis, and thermogravimetric analysis. FT-IR (KBr pellet, cm^{-1}): ν = 3419(s), 1658(m), 1602(s), 1540(m), 1417(s), 1098(w), 1018(w), 963(m), 857(w), 795(w), 711(w), 774(w), 723(m), 481(m).

NUPF-2Yb: Yield: ~16 mg (81 %, based on porphyrin). Anal. Calcd for $C_{144}H_{97}N_{12}O_{41}Yb_9 \cdot 8H_2O \cdot 10DMF$: C, 41.11; H, 3.63; N, 6.06 %, Found: C, 41.48; H, 3.82; N, 6.15 %. The overall formula of NUPF-2Yb was determined by X-ray crystallography, elemental analysis, and thermogravimetric analysis. FT-IR (KBr pellet, cm^{-1}): ν = 3399(s), 1605(m), 1541(m), 1419(s), 1176(w), 1105(w), 1020(w), 966(m), 854(w), 796(w), 771(w), 723(w), 480(m).

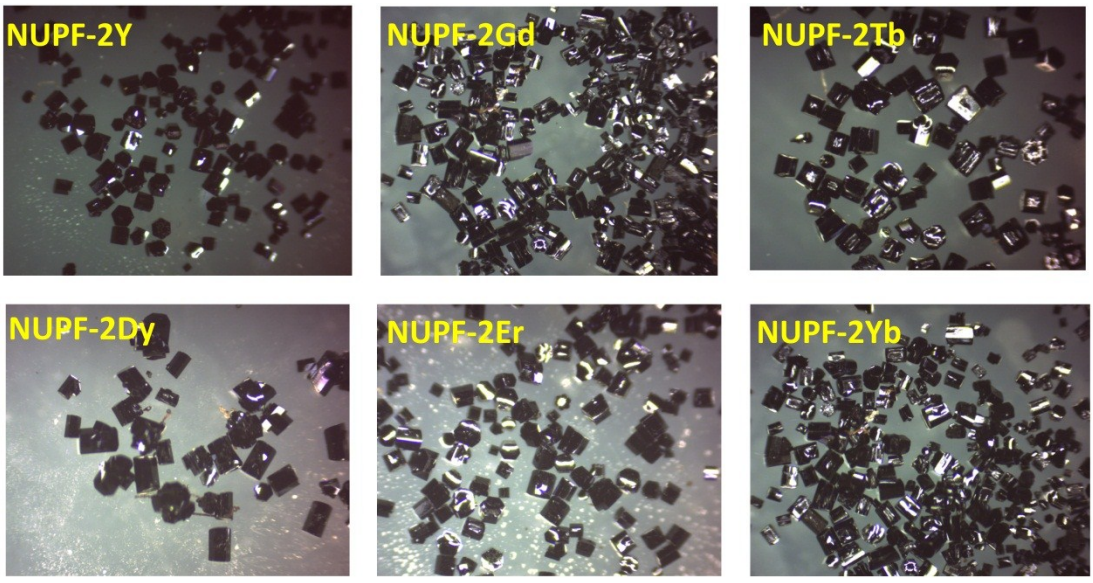

Fig. S1 Optical microscopy images of the obtained NUPF-2M crystals.

S3. Scale-up synthesis of NUPF-2M assisted by microwave reaction

All target NUPF-2M powders could be obtained by using similar protocol, therefore only the preparation of NUPF-2Y as a representative is described in detail.

Typically, 150 mg of TCPP and 12 g of 2-fluorobenzoic acid were added into 30 mL DMF in a round-bottom flask and sonicated for ten minutes for dissolution. Subsequently, 570 mg of $Y(NO_3)_3 \cdot 6H_2O$ and 7.5 mL deionized water were added to the solution and further sonicated for ten minutes. The mixture was heated by a microwave synthesizer (LWMC-201 from Nanjing Robiot Co., Ltd) at 130 Watt for 6 hours. The product was obtained by centrifugation and washed with DMF and EtOH several times. Yield: 260 mg, 85% based on porphyrin ligand.

S4. Crystallography and general comments on the CHECKCIF report.

A single crystal of NUPF-2M was isolated from the mother liquor and mounted on the sample holder via a nylon loop imbed in Paratone-N. All the X-ray diffraction data of NUPF-2M were collected on a Bruker D8 Venture diffractometer outfitted with a PHOTON-100 CMOS detector using monochromatic microfocus MoKα radiation (λ= 0.71073 Å) that was operated at 50 kV and 40 mA at 123 K by chilled nitrogen flow controlled by a KRYOFLEX II low temperature attachment. Unit cell determination was performed in the Bruker SMART APEX III software suite. The data sets were reduced and a multi-scan spherical absorption correction was implemented in the SCALE interface.[3] The structures were solved with direct methods and refined by the full-matrix least-squares method in the SHELXL-97 program package.[4] The contribution of disordered solvent molecules was treated as diffuse using SQUEEZE procedure implemented in PLATON.[5] Crystallographic data for NUPF-2M described in this paper have been deposited with the Cambridge Crystallographic Data Center (CCDC) as supplementary publication (CCDC-1490360 for NUPF-2Y, CCDC-1490362 for NUPF-2Yb, CCDC-1490366 for NUPF-2Dy, CCDC-1490367 for NUPF-2Er, CCDC-1490368 for NUPF-2Gd, CCDC-1490369 for NUPF-2Tb). Copy of the data can be obtained free of charge on application to CCDC.

General comments on the CHECKCIF reports.

It is a unique and frequently-encountered phenomenon in MPFs that when performing the X-ray diffraction analysis, the diffraction (especially in high angles) was weak. In some cases, such limited diffraction even could not be improved by using synchrotron radiation.[6] Besides the weak X-ray diffraction at high angles, there exits many disordered parts (phenyl ring, metal cluster, coordination water, *etc.*) and

large structural voids containing disordered solvents in the structures of NUPF-2M. Thus, some alerts are present in the CHECKCIF report and the corresponding responses are imbedded in the CIF file. We are confident the structural characterization is valid. Some common alerts and response are present as follows:

RFACR01_ALERT_3_B The value of the weighted R factor is > 0.35

Weighted R factor given 0.430

Response: We made several attempts to obtain better quality data for this structure. However, due to the existence of many disordered parts (phenyl ring, metal cluster, coordination water, etc.) and the weak X-ray diffraction *etc.* the R2 value is high. This structure is similar with other 5 structures of NUPF-2 series. We are confident the structural characterization is valid.

PLAT342_ALERT_3_B Low Bond Precision on C-C Bonds..... 0.02125 Ang.

Response: This problem arises from the weak X-ray diffraction of the crystal at high angles.

PLAT420_ALERT_2_B D-H Without Acceptor *O5 -- *H5 ... Please Check

Response: This problem may arise from the disordered nature of O5 and H5 atoms.

S5. Simulated and as-synthesized PXRD patterns of NUPF-2M.

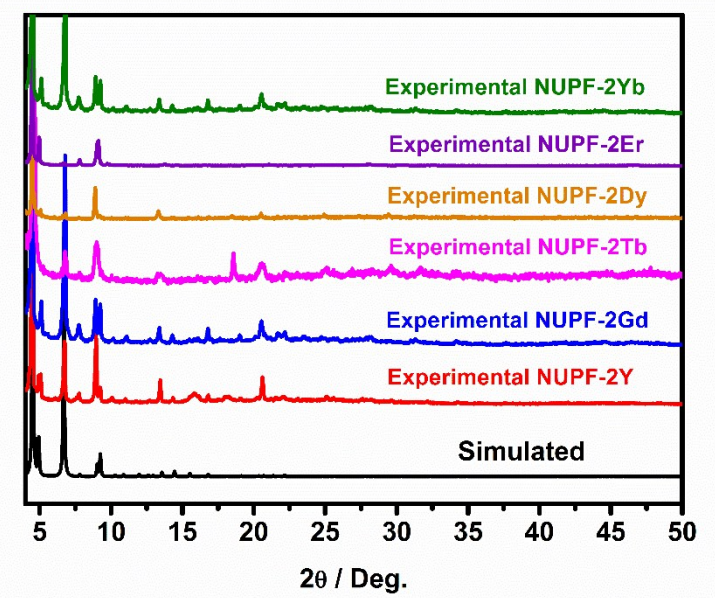

Fig. S2 PXRD patterns of NUPF-2M simulated and as-synthesized.

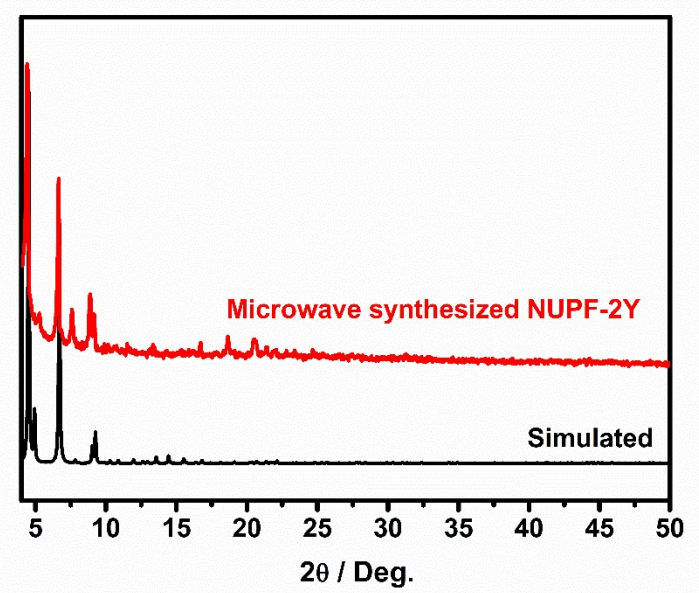

Fig. S3 Representative PXRD patterns of NUPF-2Y synthesized by microwave reaction.

S6. Comparison of the RE_9 cluster found in NUPF-2M and Zr_6 cluster in PCN-223.

The overall structure of NUPF-2M was similar to the recently reported Zr-MPF PCN-223,[7] for example, all porphyrin ligands in both structures are 4-connected and the metal clusters served as 12-connected structural nods; both structures have similar channels. Though the two types of clusters seemly constitute 18 atoms, the Zr atoms in PCN-223 are 3-fold disordered and the overall formula was determined to be Zr_6. While in the nonanuclear RE cluster in NUPF-2M, the RE atoms were disordered over two positions with 1:1 occupancy ratio, giving the overall RE_9 cluster that make it possess truncated dodeca-pyramid geometry (Fig. S4).

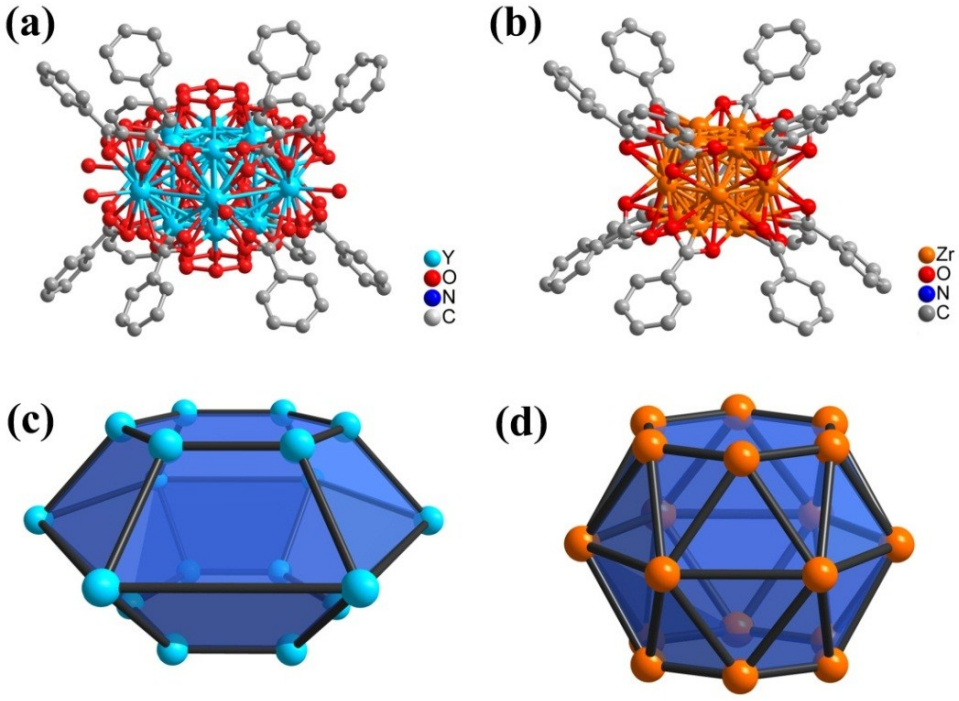

Fig. S4 (a) 2-fold disordered RE_9 clusters found in NUPF-2M (RE = Y, Yb, Tb, Gd, Er, Dy). (b) 3-fold disordered Zr_6 cluster found in PCN-223. (c) and (d) Simplified Y_9 and Zr_6 cluster.

S7. FT-IR spectroscopy of NUPF-2M.

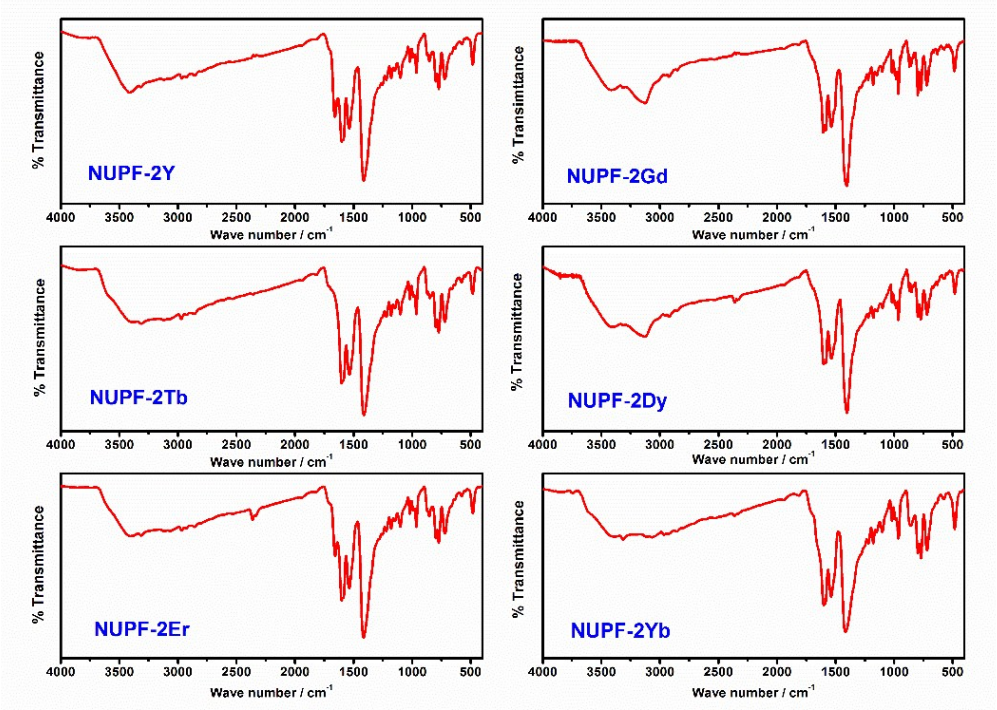

Fig. S5 FT-IR spectra of NUPF-2M.

S8. TGA profile of NUPF-2M.

Thermogravimetric analyses of the NUPF-2M were conducted from room temperature to 800 °C under N_2 atmosphere. The six NUPF-2M exhibit similar thermal behaviors. The weight losses from room temperature to *ca.* 180 °C correspond to the release of solvent molecules that were trapped in the crystal pores and/or absorbed on the crystal surfaces (five H_2O and twelve DMF for NUPF-2Y, ~21.87%, calcd 21.2%; nine H_2O and fifteen DMF for NUPF-2Gd, ~23.61%, calcd 23.72%; nine H_2O and teen DMF for NUPF-2Tb, ~17.87%, calcd 17.93%; six H_2O and seven DMF for NUPF-2Dy, ~13.57%, calcd 13.07%; six H_2O and nine DMF for NUPF-2Er, ~15.3%, calcd 15.5%; eight H_2O and ten DMF for NUPF-2Yb, ~17.1%, calcd 17.2%). A plateau up to *ca.* 500 °C was followed, implying that NUPF-2M was stable up to 500 °C. After the plateau, NUPF-2M began to decompose. The high thermal stability of NUPF-2M was further verified by checking the PXRD patterns of the samples, which were heated at 400 °C under Ar for 30 min (see main text).

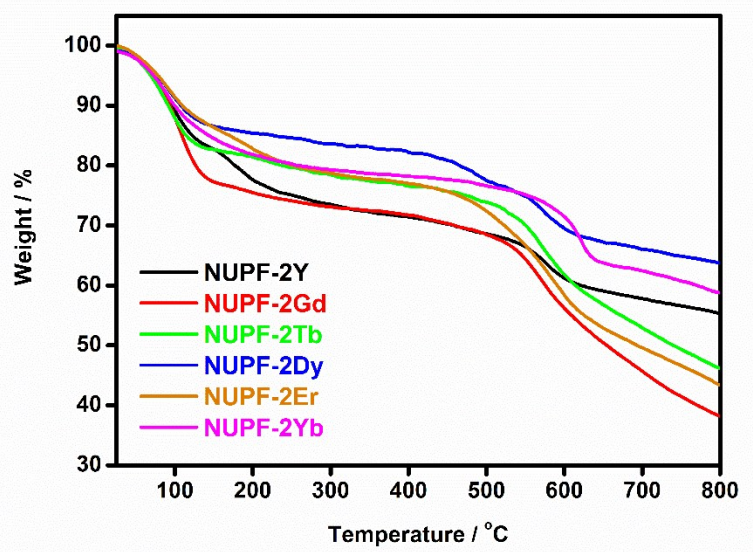

Fig. S6 TGA profiles of NUPF-2M measured from room temperature to 800 °C at a ramp rate of 10 °C / min under N_2 with a 100 mL / min flow speed.

S9. Solid-state UV-Vis spectra of NUPF-2M.

All solid-state UV-Vis spectra of NUPF-2M were similar. An intense absorption band at 370 nm and four smaller bands at ca. 501, 538, 589, 649 nm were observed and these bands could be ascribed to the Soret band and Q bands of porphyrin, respectively.

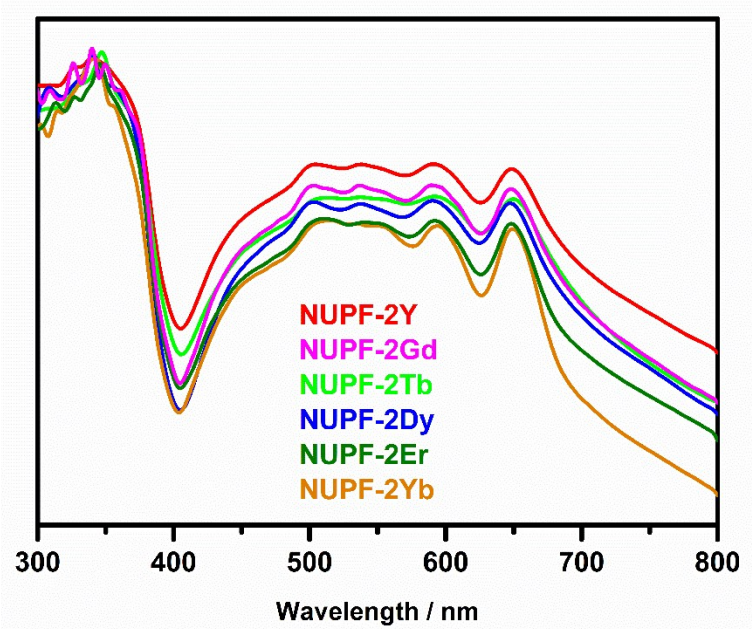

Fig. S7 Solid-state UV-Vis spectra of NUPF-2M.

S10. Gas adsorption analysis.

Sample activation: the freshly-prepared samples of NUPF-2M were soaked in MeOH for solvent exchanging, with MeOH refreshed every 12 hours. The procedure was repeated six times. Then the samples were soaked in CH_2Cl_2 for further solvents exchanging, with CH_2Cl_2 refreshed every 12 hours and repeated six times. Super-critical carbon dioxide (SCD) activation technique was then applied to activate NUPF-2M. The samples were transferred into an SFT HPR-100 reactor. The pressure and temperature gradually rose up to 1400 psi and 40 °C, respectively, and were maintained for 2 hours. The pressure was then released slowly during a period of 1 hour while temperature was still kept at 40 °C. This procedure was repeated three times. The activated samples were further activated in the analysis tube under vacuum using the “degas” function of the adsorption analyzer at 150 °C for 8 h.

Table S1 BET and Langmuir surface areas of NUPF-2M derived from N_2 adsorptions.

Sample	BET surface area (m^2/g)	Langmuir surface area (m^2/g)
NUPF-2Y	1948	2607
NUPF-2Gd	1695	2239
NUPF-2Tb	1608	2120
NUPF-2Dy	1535	2040
NUPF-2Er	1394	1834
NUPF-2Yb	1219	1603

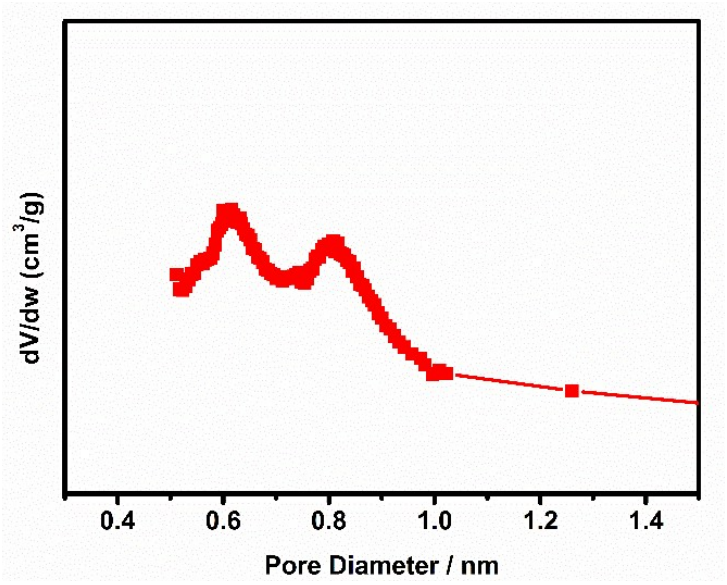

Fig. S8 Pore size distribution for NUPF-2Y using data measured with N_2 at 77K. Since the isostructural nature of NUPF-2M, only NUPF-2Y was present as a representative.

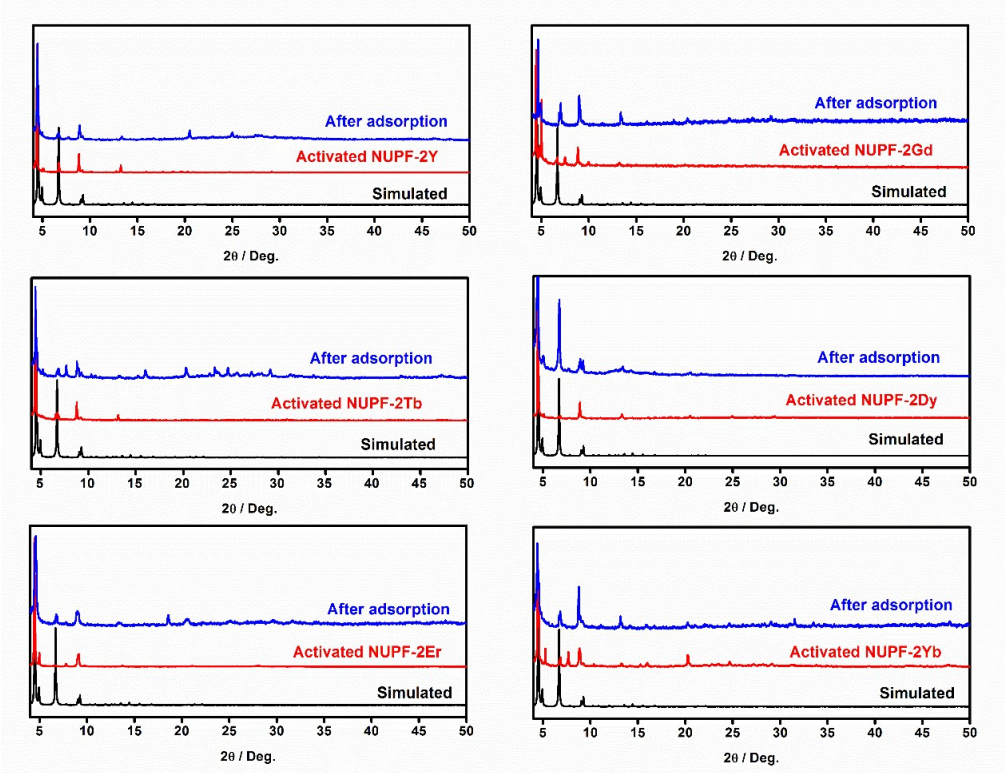

Fig. S9 PXRD patterns of NUPF-2M before and after N_2 adsorption measurements.

S11. PXRD patterns of NUPF-2M at different conditions.

About 15 mg of sample was soaked in different solutions for 3 days. After that, all the samples were filtered and washed with ethanol and anhydrous ether. For the sample in open air, about 20 mg of sample was put in a small beaker and put this beaker in ventilation place for 3 days. Then PXRD measurements were performed to check the structural stability of all samples. Since the stability of NUPF-2M is similar, only the PXRD patterns of NUPF-2Y were present as a representative.

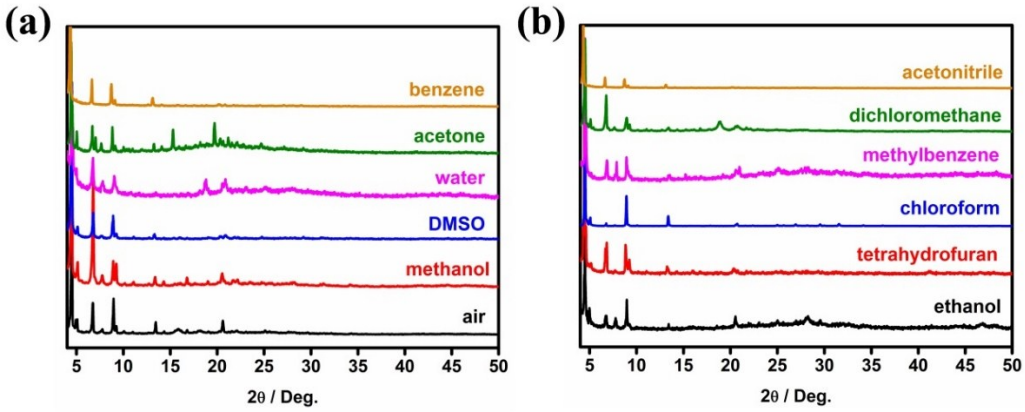

Fig. S10 PXRD patterns of NUPF-2Y under different conditions for 3 days.

S12. Metalization of NUPF-2Y with $FeCl_3$ and characterization of NUPF-2Y-FeCl.

The metallization process of NUPF-2Y by $FeCl_3$ could be accomplished by heating NUPF-2Y and $FeCl_3$ in DMF for 12 hours. Typically, 175 mg of NUPF-2Y and 233 mg of $FeCl_3$ were dispersed in 10 mL DMF. The resulting mixture was stirred and heated at 120 °C for 12 hours. After the mixture cooled to room temperature, the product was isolated by centrifugation and washed thoroughly with DMF and EtOH. As shown in Fig. S11a, the crystallinity of NUPF-2Y was well reserved after the metallization process because of its high structural stability. In the FT-IR spectra shown in Fig. S11b, the weak N-H vibration of core-freed porphyrin of NUPF-2Y was found at 963 cm^{-1}. After metalation with $FeCl_3$, this band was disappeared and a new strong absorption band at 999 cm^{-1} was observed, which is the characteristic vibration of Fe-N in metalloporphyrins,[8] suggesting that Fe was successfully inserted into the porphyrin core. For ICP-OES measurement, 10 mg of NUPF-2Y-FeCl sample was dissolved in 10 mL concentrated HNO_3 (65%) and heating at 80 °C under stirring for 1 hour, then 5 mL H_2O_2 (30%) was added dropwise and heated for other 2 hours. The resulting solution was diluted for 50 times for testing after cooled to room temperature. The results reveal NUPF-2Y-FeCl contains 14.8 mg/L Y ions and 3.11 mg/L Fe ions; the mol ratio of Y/Fe was 2.994:1, very close to the theoretical value of 3:1. Thus we believe almost all porphyrin centers of NUPF-2Y were metallized by FeCl unit.

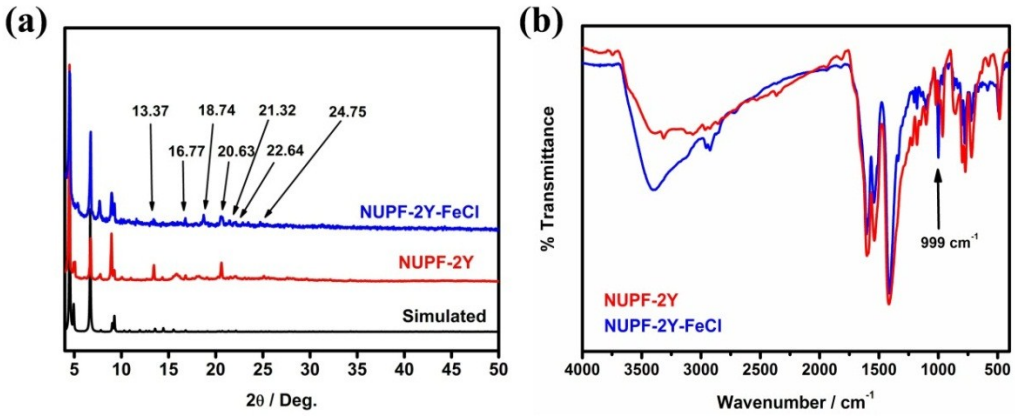

Fig. S11 (a) PXRD patterns of NUPF-2Y before and after metallization with $FeCl_3$, small peaks at 2θ = 13.37, 16.77, 18.74, 20.63, 21.32, 22.64 and 24.75 belong to (022), (032), (041), (042), (-151), (050), (043), (050) and (052) diffraction peaks of NUPF-2Y-FeCl, respectively. (b) FT-IR curves of NUPF-2Y and NUPF-2Y-FeCl.

In the UV-Vis spectra of NUPF-2Y-FeCl shown in Fig. S12, the Soret band of NUPF-2Y-FeCl was located at 373 nm, while 540 nm and 589 nm bands were ascribed to the Q bands of NUPF-2Y-FeCl. Compared with NUPF-2Y, the slight red shift of the Soret band and reduction of the Q band number from four to two were ascribed to the metallization of the porphyrin core.[9]

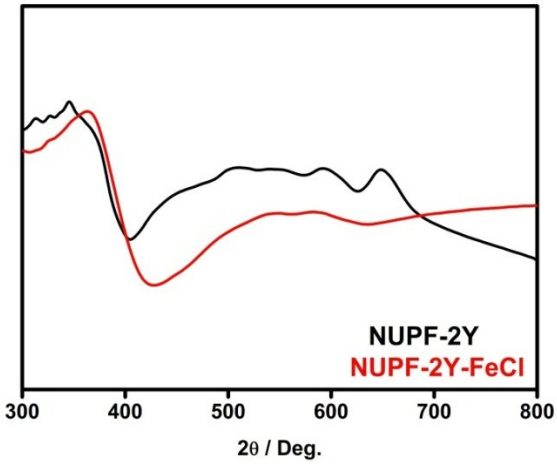

Fig S12 Solid-state UV-Vis spectra of NUPF-2Y and NUPF-2Y-FeCl.

S13. Catalytic reactions

General: Round-bottom flasks used in the catalytic reaction were dried in an oven at 120 °C prior to use. Ethyl diazoacetate (EDA),[10] Fe(TPP)Cl[2] were prepared according to literature procedures. Aniline was distilled from CaH_2 under reduced pressure. Dichloromethane was distilled from CaH_2 and purged by argon before to use. Catalyst NUPF-2Y-FeCl was dried at 150 °C under vacuum for 12 hours before to use. Other reagents and solvents were used as received from commercial sources without any further purification.

Catalytic test: In a 25 mL round-bottom flask, an amine (0.3 mmol) was dissolved in 8 mL of dichloromethane which contains 1 % mmol catalyst (3.7 mg for NUPF-2Y-FeCl and 2.1 mg for Fe(TPP)Cl, based on Fe-porphyrin unit) and high purity Ar was bubbled through the solution for 10 min. Then EDA (1.20 equiv, 0.36 mmol) in 1 mL of dichloromethane was added under Ar stream, and the reaction mixture was stirred for a given time. Upon completion of the reaction, as checked by TLC (approximately 30 min for NUPF-2Y-FeCl), the solvent was removed and the products were purified by purified by flash chromatography. For catalyst recycling test, when

the reaction was complete, the catalyst was separated by centrifugation and directly used for another catalytic run.

CAUTION: ethyl diazoacetate (EDA) used in the catalytic experiments is potentially explosive, the operations should be carried out in a well-ventilated hood with an adequate safety shield. Besides, rapid gas release was observed during the catalytic reaction, reaction vessels should be handled with care.

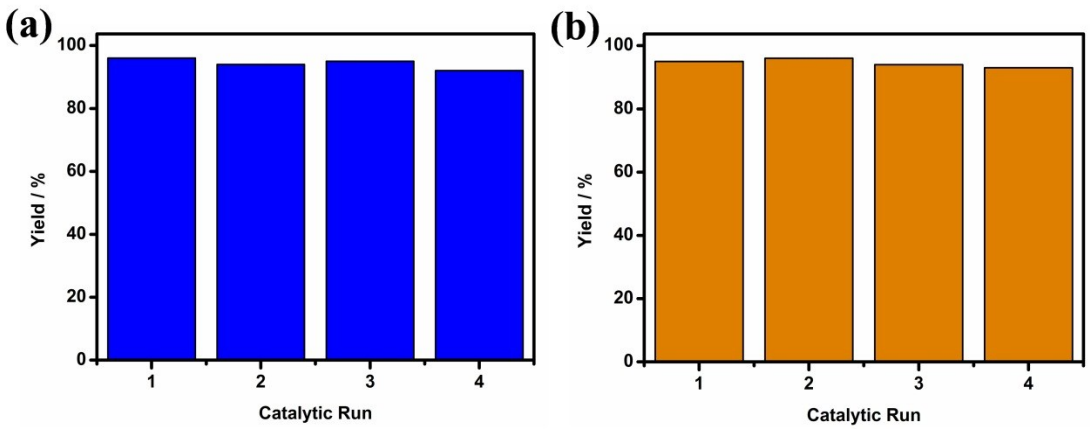

Fig. S13 The catalytic yield in the reaction of aniline as substrate (a) and 4-fluoroaniline as substrate (b), respectively.

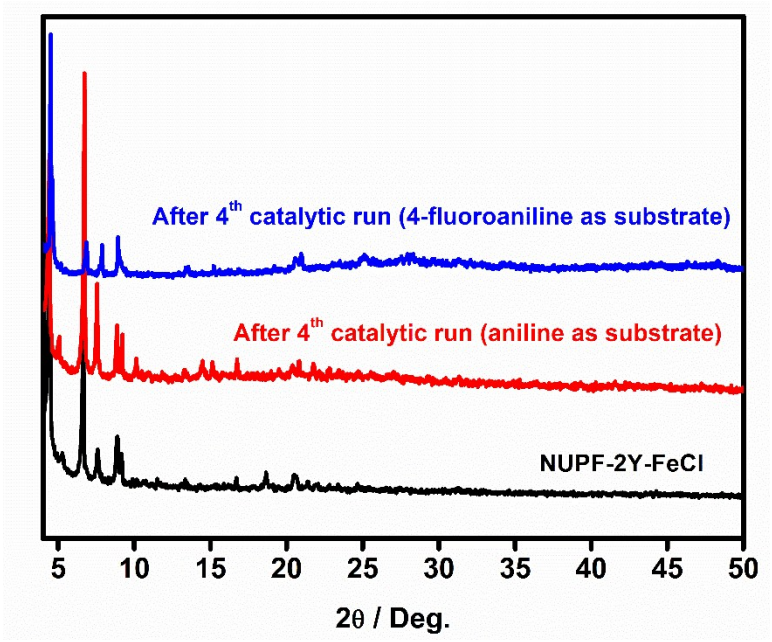

Fig. S14 PXRD patterns of NUPF-2Y-FeCl before and after 4th catalytic run (aniline and 4-fluoroaniline as substrates).

S14. ^{1}H NMR spectra.

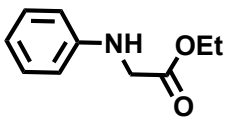

Ethyl phenylglycinate:[11] white solid, ethyl acetate/hexane = 1:10, R_f = 0.35. ^{1}H NMR ($CDCl_3$, 300 MHz), δ 7.22 (q, 2H), 6.78 (t, 1H), 6.65 (d, 2H), 4.28 (q, 2H), 3.93 (s, 2H), 1.32 (t, 3H).

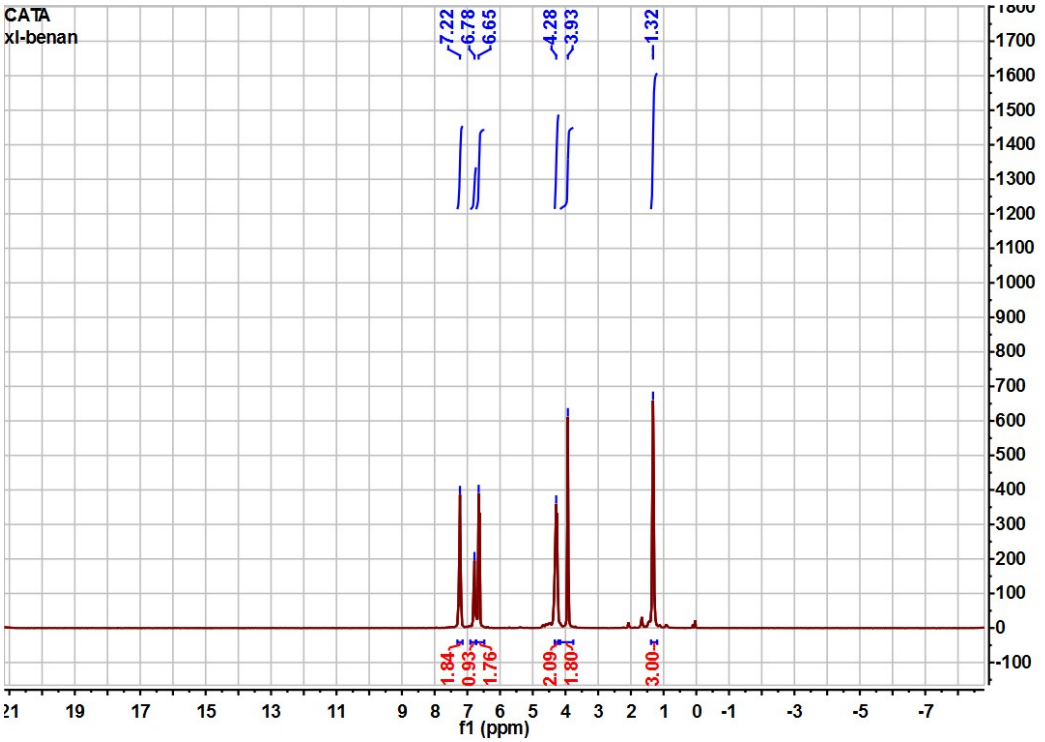

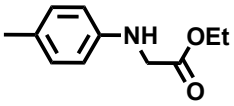

Ethyl *p*-tolylglycinate:[12] yellow solid, ethyl acetate/hexane = 1:10, R_f = 0.4. ^{1}H NMR ($CDCl_3$, 300 MHz), δ 6.99 (d, 2H), 6.54 (d, 2H), 4.42 (q, 2H), 3.87 (s, 2H), 2.23 (s, 3H), 1.28 (t, 3H).

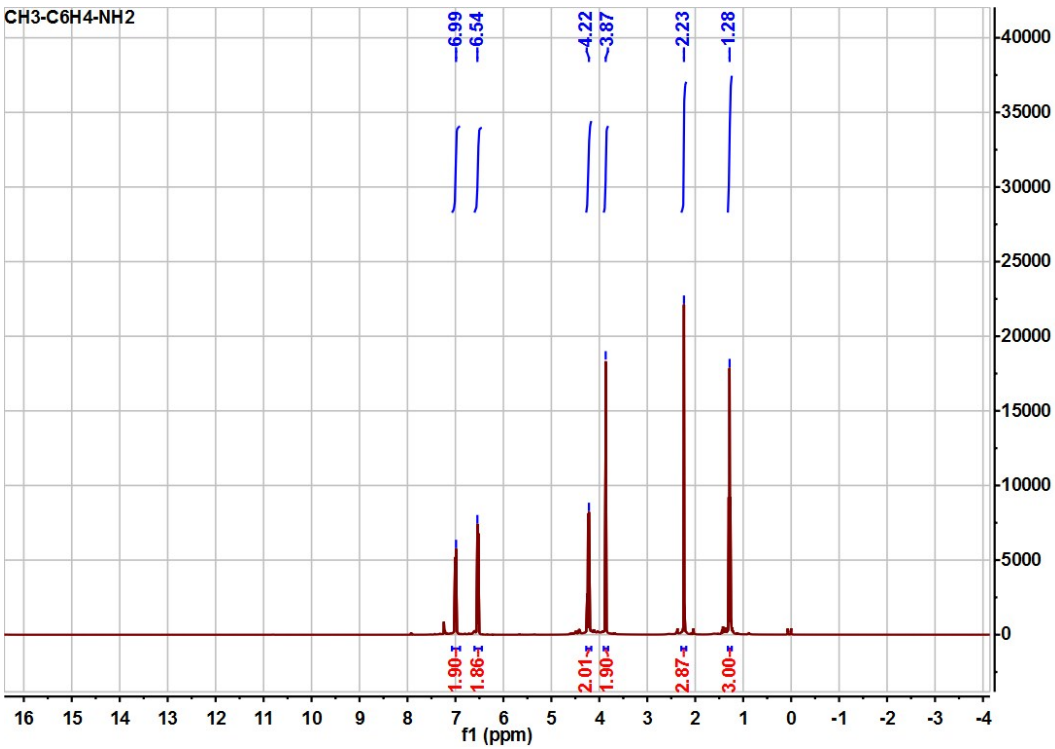

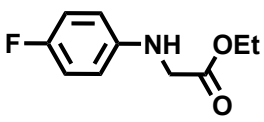

Ethyl (4-fluorophenyl)glycinate:[12] colorless crystals, ethyl acetate/hexane = 1:5, R_f = 0.5. ^{1}H NMR ($CDCl_3$, 300 MHz), δ 6.90 (d, 2H), 6.55 (q, 2H), 4.23 (q, 3H), 3.86 (s, 2H), 1.29 (t, 3H).

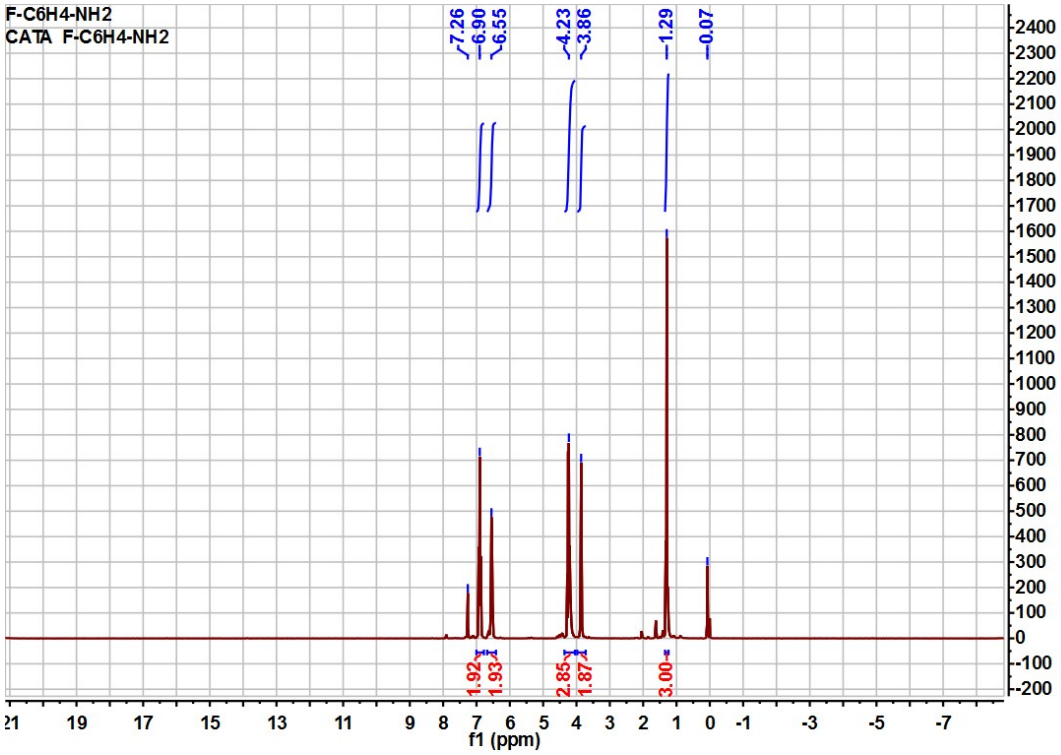

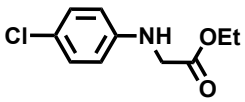

Ethyl (4-chlorophenyl)glycinate:[12] white solid, ethyl acetate/hexane = 1:10, R_f = 0.3. ^{1}H NMR ($CDCl_3$, 300 MHz), δ 7.12 (d, 2H), 6.54 (d, 2H), 4.25 (q, 3H), 3.87 (d, 2H), 1.29 (q, 3H).

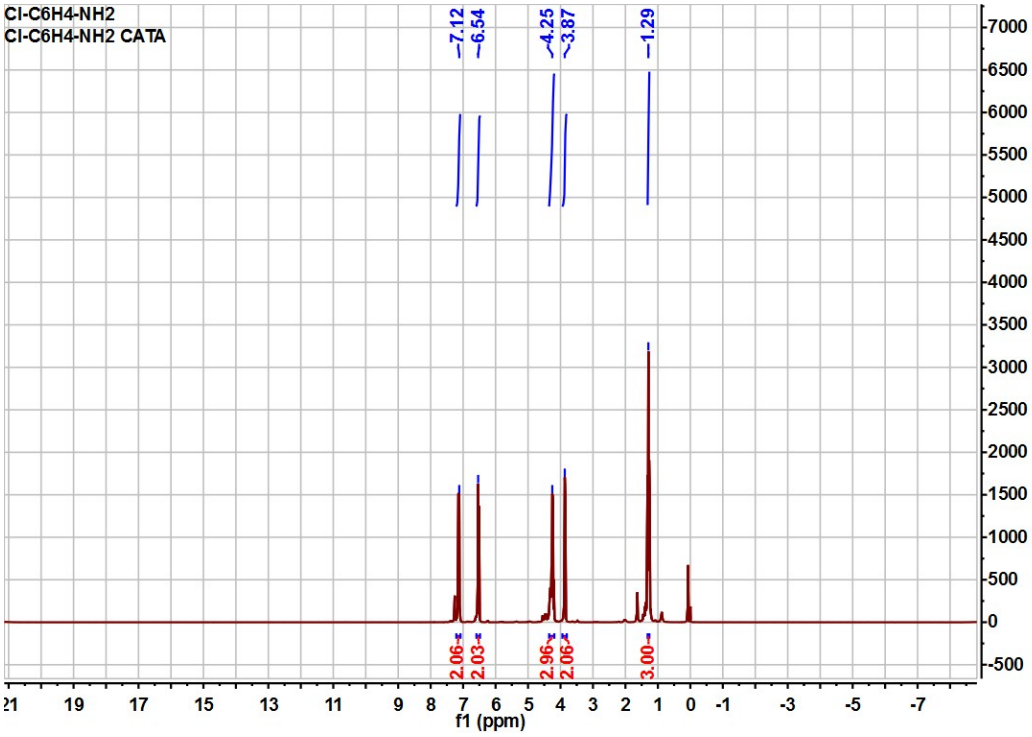

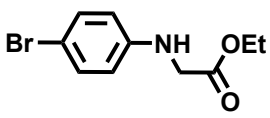

Ethyl (4-bromophenyl)glycinate:[12] white solid, ethyl acetate/hexane = 1:10, Rf = 0.4. ^{1}H NMR ($CDCl_3$, 300 MHz), δ 7.27 (d, 2H), 6.51 (d, 2H), 4.28 (q, 3H), 3.88 (d, 2H), 1.32 (q, 3H).

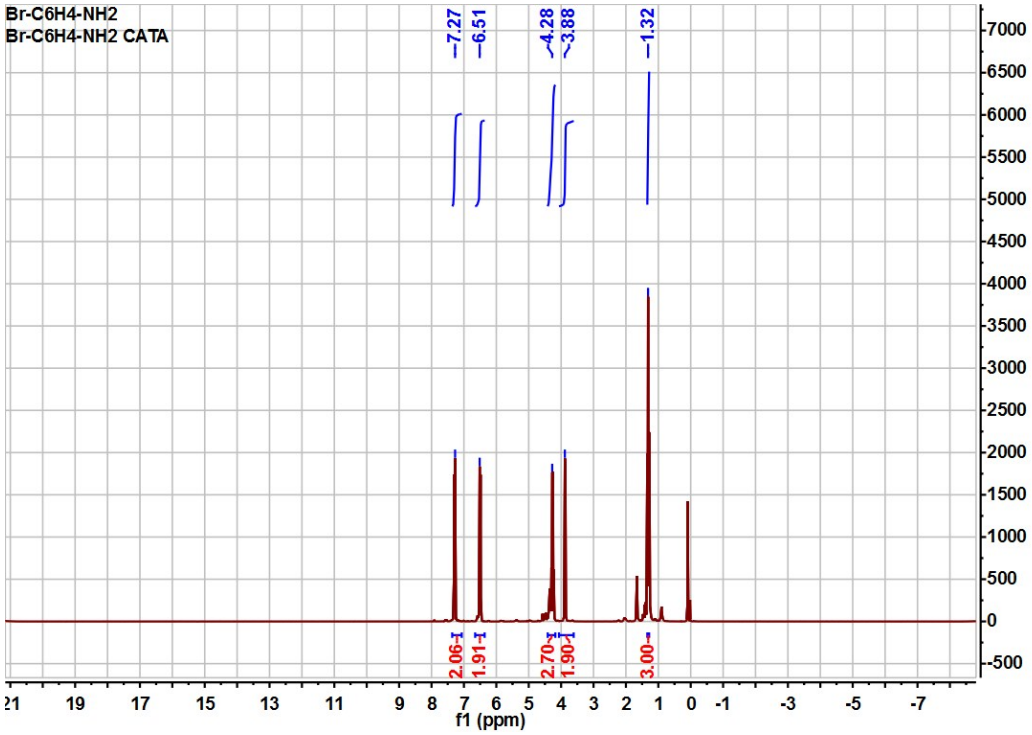

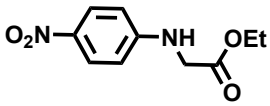

Ethyl (4-nitrophenyl)glycinate:[13] yellow solid, ethyl acetate/hexane = 2:5, R_f = 0.4. ^{1}H NMR ($CDCl_3$, 300 MHz), δ 8.08 (d, 2H), 6.53 (d, 2H), 5.13 (s, 1H), 4.27 (q, 3H), 3.98 (d, 2H), 1.31 (q, 3H).

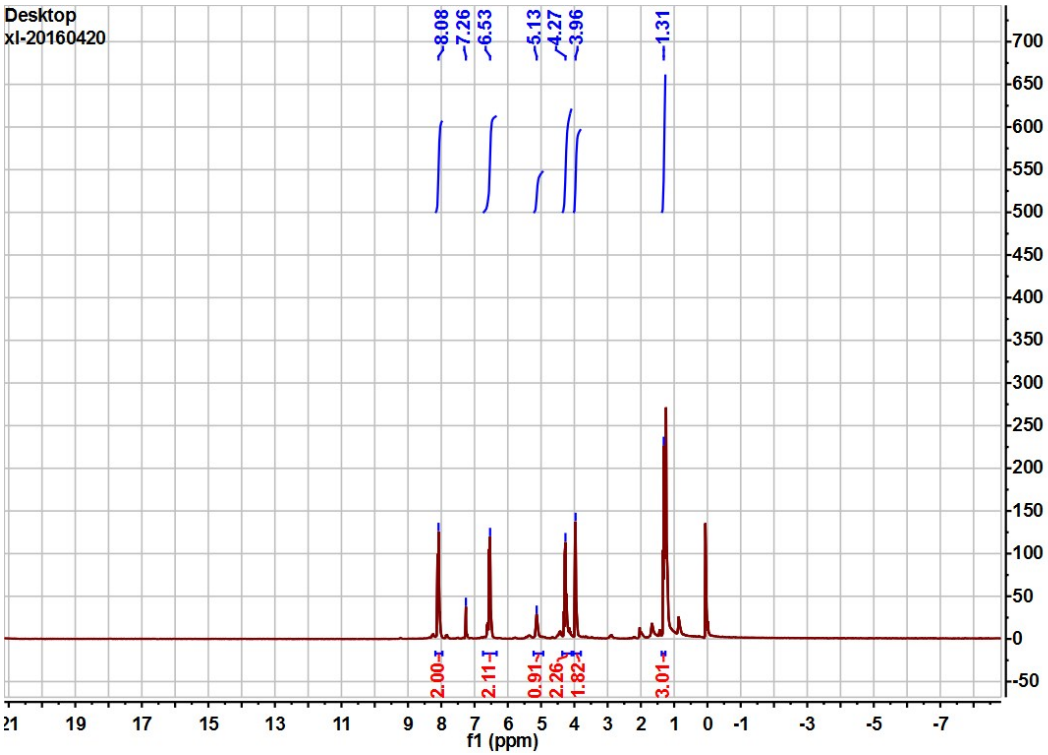

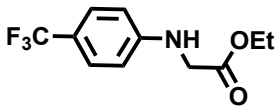

Ethyl (4-(trifluoromethyl)phenyl)glycinate:[12] while solid, ethyl

acetate/hexane = 1:10, R_f = 0.3. ^{1}H NMR ($CDCl_3$, 300 MHz), δ 7.41 (d, 2H), 6.62 (d, 2H), 4.66 (s, 1H), 4.27 (q, 2H), 3.92 (s, 2H), 1.31 (q, 3H).

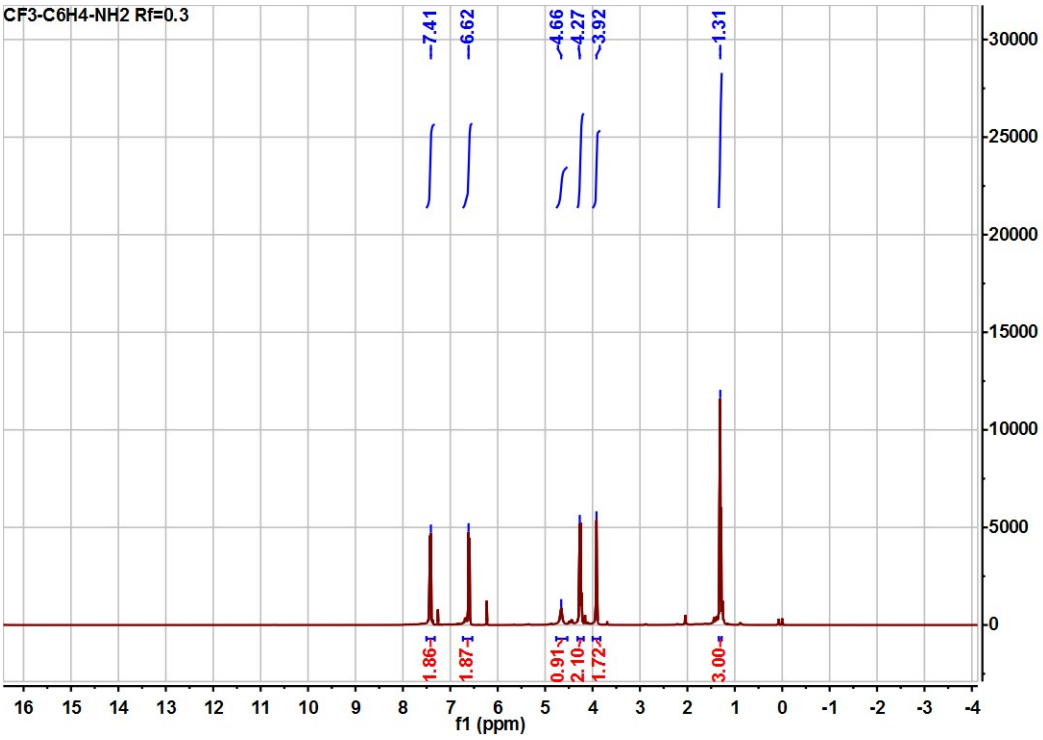

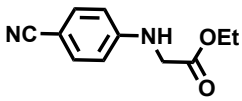

Ethyl (4-cyanophenyl)glycinate:[12] yellow solid, ethyl acetate/hexane = 2:5, R_f = 0.5. ^{1}H NMR ($CDCl_3$, 300 MHz), δ 7.46 (d, 2H), 6.58 (d, 2H), 4.87 (s, 1H), 4.28 (q, 2H), 3.94 (s, 2H), 1.33 (q, 3H).

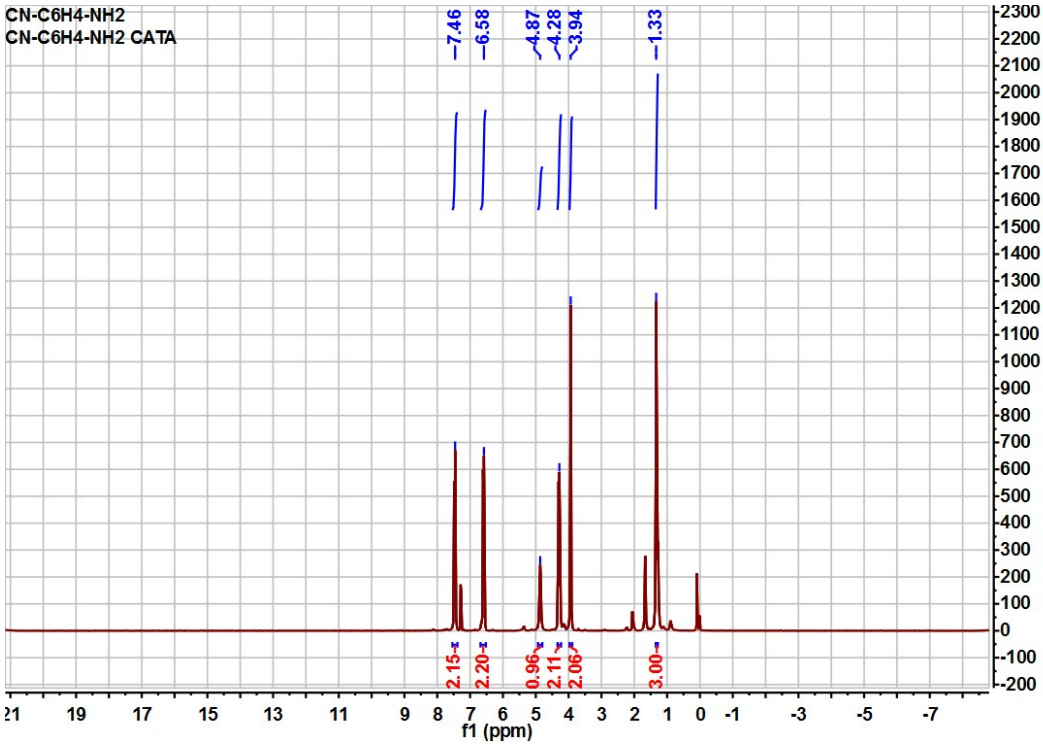

S15. GC-MS profiles of the reaction of anilinein 10 mmol scale

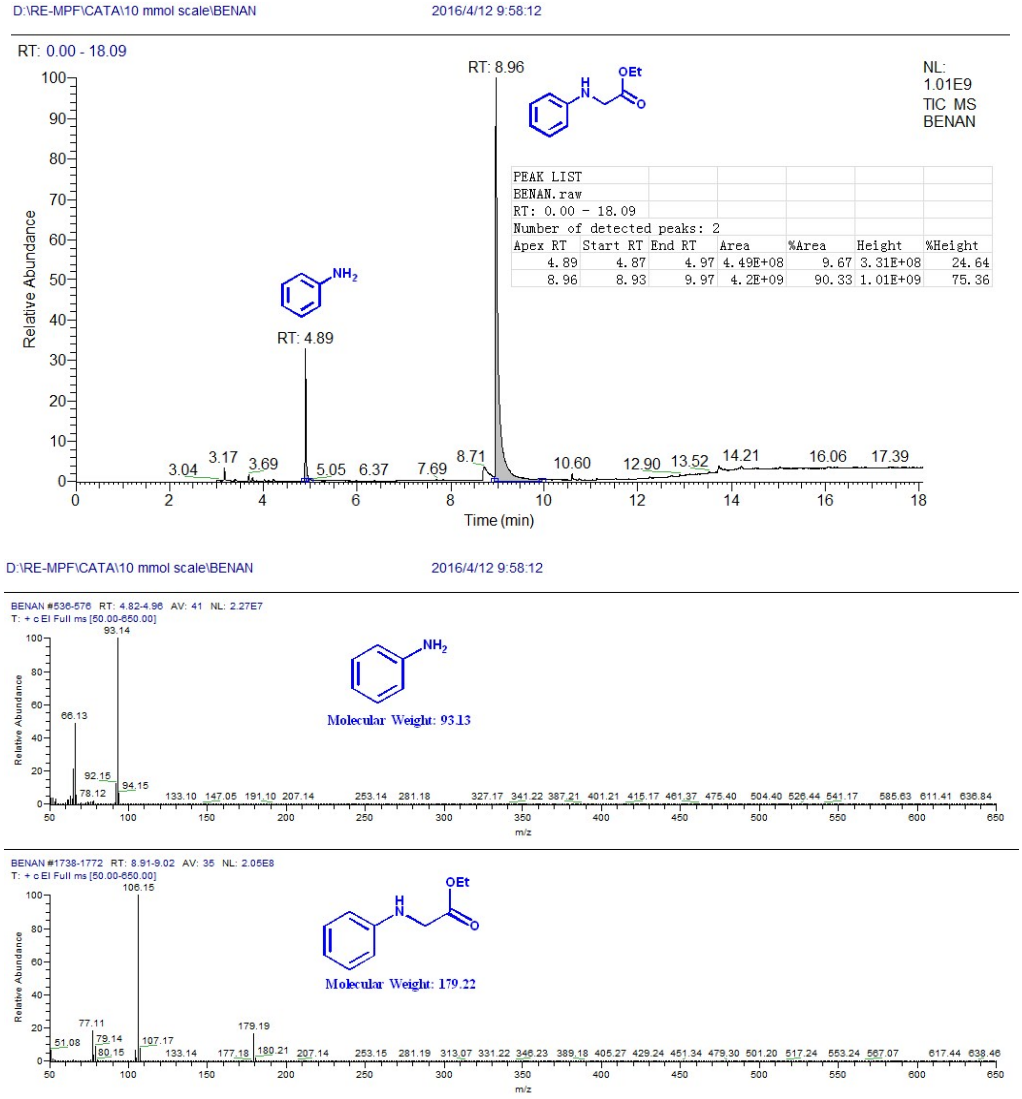

S16. Crystal data for NUPF-2M.

Compound	NUPF-2Y	NUPF-2Yb	NUPF-2Dy
CCDC number	1490360	1490362	1490366
Empirical formula	$C_{144}H_{97}N_{12}O_{41}Y_9$	$C_{144}H_{97}N_{12}O_{41}Yb_9$	$C_{144}H_{97}N_{12}O_{41}Dy_9$
Formula weight	3451.53	4208.70	4113.84
Temperature	123 K	123 K	123 K
Wavelength	0.71073 Å	0.71073 Å	0.71073 Å
Crystal system	Hexagonal	Hexagonal	Hexagonal
space group	P6/mmm	P6/mmm	P6/mmm
Unit cell dimensions	a=22.6495(13)Å α = 90°	a=22.7374(5)Å α = 90°	a=22.7374(5)Å α = 90°
	b=22.6495(13)Å β= 90 °	b=22.7374(5) Å β= 90 °	b=22.7374(5) Å β= 90 °
	c=17.9177(12) Å γ= 120 °	c=17.8238(8)Å γ= 120 °	c=17.8238(8)Å γ= 120 °
Volume	7960.3(8) $Å^3$	7980.2(4)$Å^3$	7980.2(4)$Å^3$

Z, Calculated density	1, 0.720 Mg/m^3	1, 0.876 Mg/m^3	1, 0.856 Mg/m^3
Absorption coefficient	1.658 mm^{-1}	2.646 mm^{-1}	2.116 mm^{-1}
F(000)	1724	2003	1967
Theta range for data collection	2.08 to 25.01°	2.07 to 25.05°	2.12 to 25.05°
Reflections collected / unique	57346 / 2749 [*R*(int) = 0.0547]	55858 / 2762 [R(int) = 0.0520]	55056 / 2737 [R(int) = 0.0510]
Completeness to theta = 25.05	99.9 %	99.9 %	99.0 %
Absorption correction	Semi-empirical from equivalents	Semi-empirical from equivalents	Semi-empirical from equivalents
Max. and min. transmission	0.6361 and 0.5945	0.4028 and 0.3757	0.5081 and 0.4848
Refinement method	Full-matrix least-squares on F^2	Full-matrix least-squares on F^2	Full-matrix least-squares on F^2
Data / restraints / parameters	2749 / 0 / 142	2762 / 0 / 141	2737 / 0 / 141
Goodness-of-fit on F^2	1.897	1.108	2.176
Final R indices [I>2sigma(I)]	R1 = 0.1297, wR2 = 0.3870	R1 = 0.1247, wR2 = 0.3376	R1 = 0.1393, wR2 = 0.4250
R indices (all data)	R1 = 0.1360, wR2 = 0.3931	R1 = 0.1296, wR2 = 0.3418	R1 = 0.1427, wR2 = 0.4298
Largest diff. peak and hole	2.221 and -2.992 $e.A^{-3}$	3.076 and -7.814 $e.A^{-3}$	2.752 and -6.878 $e.A^{-3}$

Compound	NUPF-2Er	NUPF-2Gd	NUPF-2Tb
CCDC number	1490367	1490368	1490369
Empirical formula	$C_{144}H_{97}N_{12}O_{41}Er_9$	$C_{144}H_{97}N_{12}O_{41}Gd_9$	$C_{144}H_{97}N_{12}O_{41}Tb_9$
Formula weight	4156.68	4066.59	4081.62
Temperature	123 K	123 K	123 K
Wavelength	0.71073 Å	0.71073 Å	0.71073 Å
Crystal system	Hexagonal	Hexagonal	Hexagonal
space group	P6/mmm	P6/mmm	P6/mmm
Unit cell dimensions	a=22.7374(5)Å α = 90°	a=22.7374(5)Å α = 90°	a=22.7374(5)Å α = 90°
	b=22.7374(5) Å β= 90 °	b=22.7374(5) Å β= 90 °	b=22.7374(5) Å β= 90 °
	c=17.8238(8)Å γ= 120 °	c=17.8238(8)Å γ= 120 °	c=17.8238(8)Å γ= 120 °
Volume	7980.2(4)$Å^3$	7980.2(4)$Å^3$	7980.2(4)$Å^3$
Z, Calculated density	1, 0.865 Mg/m^3	1, 0.846 Mg/m^3	1, 0.849Mg/m^3
Absorption coefficient	2.376 mm^{-1}	1.879 mm^{-1}	2.004 mm^{-1}

F(000)	1985	1949	1958
Theta range for data collection	2.12 to 25.05°	2.36 to 25.05°	2.07 to 25.05°
Reflections collected / unique	56263 / 2761 [R(int) = 0.0471]	57012 / 2730 [R(int) = 0.0571]	51916 / 2738 [R(int) = 0.0631]
Completeness to theta = 25.05	99.8 %	98.7 %	99.0 %
Absorption correction	Semi-empirical from equivalents	Semi-empirical from equivalents	Semi-empirical from equivalents
Max. and min. transmission	0.4500 and 0.4282	0.5592 and 0.5353	0.5848 and 0.5577
Refinement method	Full-matrix least-squares on F^2	Full-matrix least-squares on F^2	Full-matrix least-squares on F^2
Data / restraints / parameters	2761 / 0 / 141	2730 / 0 / 141	2738 / 0 / 141
Goodness-of-fit on F^2	1.039	2.413	2.360
Final R indices [I>2sigma(I)]	R1 = 0.1274, wR2 = 0.3201	R1 = 0.1573, wR2 = 0.4669	R1 = 0.1765, wR2 = 0.4736
R indices (all data)	R1 = 0.1313, wR2 = 0.3229	R1 = 0.1604, wR2 = 0.4711	R1 = 0.1836, wR2 = 0.4808
Largest diff. peak and hole	2.011 and -6.095 e.A^{-3}	2.773 and -7.346e.A^{-3}	3.127 and -6.832e.A^{-3}

S17. References

1. D. Feng, Z.-Y. Gu, J.-R. Li, H.-L. Jiang, Z. Wei and H.-C. Zhou, *Angew. Chem. Int. Ed.*, 2012, **51**, 10307-10310; L. Maqueira, A. Iribarren, A. C. Valdés, C. P. de Meloc and C. G. dos Santos, *J. Porphyrins and Phthalocyanines*, 2012, **16**, 267-272.
2. Z. Sun, Y. She and R. Zhong, *Front. Chem. Eng. China*, 2009, **3**, 457-461.
3. C. H. Gorbitz, *Acta Crystallog. B*, 1999, **55**, 1090-1098.
4. G. M. Sheldrick, *Acta Crystallog. A*, 2008, **64**, 112-122.
5. A. Spek, *J. Appl. Crystallog.*, 2003, **36**, 7-13.
6. X.-S. Wang, M. Chrzanowski, W.-Y. Gao, L. Wojtas, Y.-S. Chen, M. J. Zaworotko and S. Ma, *Chem. Sci.*, 2012, **3**, 2823-2827; L. Meng, Q. Cheng, C. Kim, W.-Y. Gao, L. Wojtas, Y.-S. Chen, M. J. Zaworotko, X. P. Zhang and S. Ma, *Angew. Chem. Int. Ed.*, 2012, **51**, 10082-10085.
7. D. Feng, Z.-Y. Gu, Y.-P. Chen, J. Park, Z. Wei, Y. Sun, M. Bosch, S. Yuan and H.-C. Zhou, *J. Am. Chem. Soc.*, 2014, **136**, 17714-17717.
8. X. Lu, Z. Geng, Y. Wang, B. Lv and J. Kang, *Synth. React. Inorg. Met-Org. Chem.*, 2002, **32**, 843-851;D. W. Thomas and A. E. Martell, *J. Am. Chem. Soc.*, 1959, **81**, 5111-5119.
9. R. J. P. Williams, *Chem. Rev.*, 1956, **56**, 299-328; M. Jahan, Q. Bao and K. P. Loh, *J. Am. Chem. Soc.*, 2012, **134**, 6707-6713.
10. S. A. Moore and D. E. G. Shuker, *J. Labelled. Comp. Radiopharm.*, 2011, **54**, 855-858.
11. I. Aviv and Z. Gross, *Chem. Eur. J.*, 2008, **14**, 3995-4005.
12. R. Rohlmann, T. Stopka, H. Richter and O. Garćia Mancheño, *J. Org. Chem.*, 2013, **78**, 6050-6064.
13. G. Sreenilayam and R. Fasan, *Chem. Commun.*, 2015, **51**, 1532-1534.